Published in final edited form as:

Cancer Res. 2016 May 15; 76(10): 2954–2963. doi:10.1158/0008-5472.CAN-15-2121.

The EGF receptor promotes the malignant potential of glioma by regulating amino acid transport system xc(−)

Kenji Tsuchihashi[1,2], **Shogo Okazaki**[1], **Mitsuyo Ohmura**[3], **Miyuki Ishikawa**[1], **Oltea Sampetrean**[1], **Nobuyuki Onishi**[1], **Hiroaki Wakimoto**[4], **Momoko Yoshikawa**[1], **Ryo Seishima**[1], **Yoshimi Iwasaki**[1], **Takayuki Morikawa**[3,5], **Shinya Abe**[6], **Ayumi Takao**[6], **Misato Shimizu**[6], **Takashi Masuko**[6], **Motoo Nagane**[7], **Frank Furnari**[8], **Tetsu Akiyama**[9], **Makoto Suematsu**[3,10], **Eishi Baba**[2], **Koichi Akashi**[2], **Hideyuki Saya**[1], and **Osamu Nagano**[1]

[1]Division of Gene Regulation, Institute for Advanced Medical Research, School of Medicine, Keio University, Shinjuku-ku, Tokyo 160-8582, Japan

[2]Department of Medicine and Biosystemic Science, Kyushu University Graduate School of Medical Sciences, Higashi-ku, Fukuoka 812-8582, Japan

[3]Department of Biochemistry, School of Medicine, Keio University, Shinjuku-ku, Tokyo 160-8582, Japan

[4]Department of Neurosurgery, Massachusetts General Hospital, Harvard Medical School, Boston, MA 02114, USA

[5]Department of Stem Cell Biology, Research Institute, National Center for Global Health and Medicine, Tokyo 162-8655, Japan

[6]Cell Biology Laboratory, Department of Pharmaceutical Sciences, Faculty of Pharmacy, Kinki University, Higashiosaka, Osaka 577-8502, Japan

[7]Department of Neurosurgery, Kyorin University Faculty of Medicine, Mitaka, Tokyo 181-8611, Japan

[8]Ludwig Institute for Cancer Research, University of California at San Diego, La Jolla, CA 92093, USA

[9]Laboratory of Molecular and Genetic Information, Institute of Molecular and Cellular Biosciences, The University of Tokyo, Bunkyo-ku, Tokyo, Japan

[10]Japan Science and Technology Agency (JST), Exploratory Research for Advanced Technology (ERATO), Suematsu Gas Biology Project, Tokyo 160-8582, Japan

Abstract

Extracellular free amino acids contribute to the interaction between a tumor and its microenvironment through effects on cellular metabolism and malignant behavior. System xc(−) is composed of xCT and CD98hc subunits and functions as a plasma membrane antiporter for the

Address correspondence to: Osamu Nagano, DDS, PhD, Division of Gene Regulation, Institute for Advanced Medical Research, Keio University School of Medicine, 35 Shinanomachi, Shinjuku-ku, Tokyo 160-8582, Japan. Tel.: +81-3-5363-3983. Fax: +81-3-5363-3982. ; Email: osmna@sb3.so-net.ne.jp.

Conflict of interest: None of the authors have any relevant conflicts of interest pertaining to the studies and data in this manuscript.

uptake of extracellular cystine in exchange for intracellular glutamate. Here we show that the epidermal growth factor receptor (EGFR) interacts with xCT and thereby promotes its cell surface expression and function in human glioma cells. EGFR-expressing glioma cells manifested both enhanced antioxidant capacity as a result of increased cystine uptake as well as increased glutamate which promotes matrix invasion. Imaging mass spectrometry also revealed that brain tumors formed in mice by human glioma cells stably overexpressing EGFR contained higher levels of reduced glutathione compared with those formed by parental cells. Targeted inhibition of xCT suppressed the EGFR-dependent enhancement of antioxidant capacity in glioma cells as well as tumor growth and invasiveness. Our findings establish a new functional role for EGFR in promoting the malignant potential of glioma cells through interaction with xCT at the cell surface.

Keywords

epidermal growth factor receptor (EGFR); xCT; glutamate; matrix invasion; glioma

Introduction

An emerging concept relating to the interaction between a tumor and its microenvironment is that external amino acids support the survival and propagation of cancer cells (1). Cancer cells manifest an increased demand for and consumption of amino acids as a result of their altered metabolism (2, 3), and they often exhibit high levels of expression of cell surface transporters and receptors for amino acids (4). System xc(−), which consists of a light-chain subunit (xCT, SLC7A11) and a heavy-chain subunit (CD98hc, SLC3A2), is a major plasma membrane antiporter that mediates the cellular uptake of cystine in exchange for intracellular glutamate. Surface expression of xCT increases the uptake of cystine required for intracellular synthesis of reduced glutathione (GSH) (5, 6) and is thus an important determinant of intracellular redox balance in cancer cells (7, 8). We recently showed that variant isoforms of CD44 (CD44v), but not the standard isoform (CD44s), interact with and stabilize xCT and thereby potentiate the ability of cancer cells to defend themselves against reactive oxygen species (ROS) (6, 9, 10). In addition to CD44v-expressing cancer cells, several cancer cell types including glioma cells that do not express CD44v (11, 12) have also recently been shown to manifest a high level of surface xCT expression and consequent enhanced uptake of extracellular cystine (13, 14). However, the mechanism by which surface xCT expression and the consequent cystine uptake and GSH synthesis is regulated in a manner independent of CD44v in CD44s-expressing cancer cells has remained unknown.

Extracellular glutamate has been shown to play a key role in malignant behavior of cancer cells including cell proliferation and matrix invasion (15, 16). Malignant glioma cells that express CD44s (but not CD44v) have been shown to release large amounts of glutamate in the brain (11, 17, 18), suggesting that system xc(−) is activated in CD44s-expressing glioma cells and generates a glutamate-rich microenvironment. However, the mechanism of xCT regulation in glioma cells and the functional relevance of system xc(−) to the interaction of these cells with their microenvironment have not been elucidated

We have now investigated the molecular mechanism by which surface xCT expression is regulated in glioma cells that express CD44s (but not CD44v) as well as the functional role of amino acids including cystine and glutamate in the promotion of the malignant potential of glioma.

Materials and Methods

Cell culture

T98G, U87MG, and U251MG cells were obtained from American Type Culture Collection (Manassas, VA) and KNS42 and Becker cells were from JRCB Cell Bank (Osaka, Japan) in 2014. These cells were maintained under 5% CO_2 at 37°C in Dulbecco's modified Eagle's medium (DMEM) containing glucose at 4.5g/l (Nacalai, Kyoto, Japan) and supplemented with 10% FBS. All cell lines were used within 6 months to 1year upon receipt of cells, and characterization by STR analysis was performed before use. Human primary glioblastoma MGG18 and GB2 cells were obtained from Massachusetts General Hospital and The University of Tokyo in October and November of 2015, respectively, and were cultured as previously described (19, 20).

Drug treatment in vivo

U87MG or U87MG-EGFR cells (2×10^6) were implanted subcutaneously in the flank of nude mice. The mice were then injected intraperitoneally with saline, sulfasalazine (250 mg/kg), cisplatin (2 mg/kg), or both drugs, with saline and sulfasalazine being injected once a day and cisplatin injected once every 3 days for 14 days. All animal experiments were performed in accordance with protocols approved by the Ethics Committee of Keio University.

Measurement of reduced and oxidized glutathione, cysteine content, and cystine uptake

The intracellular contents of reduced (GSH) and oxidized (GSSG) glutathione and of cysteine in U87MG and U87MG-EGFR cells were measured by capillary electrophoresis combined with mass spectrometry (Agilent Technology, Tokyo, Japan). For measurement of cystine uptake, cells were incubated for 5 min at 37°C with DMEM supplemented with $^{15}N_2$-L-cystine (>98% purity, 0.0938 g/l; Cambridge Isotope Laboratories, Andover, MA), lysed, and assayed for $^{15}N_1$-cysteine incorporation.

In vitro invasion assay

The cell suspensions of MGG18 or GB2 cells (200 μl) were transferred to the upper chamber of inserts with a pore size of 8.0 μm whose bottom surface was coated with laminin (Corning). Sulfasalazine (200 μM) or glutamate (250 μM) was added to the medium in both upper and lower chambers. After culture for 12 h, the number of cells on the lower surface of each insert was determined.

Imaging mass spectrometry

U87MG cells (2×10^5) were injected into the left hemisphere of NOD/SCID mice, and, after 7 days, U87MG-EGFR cells (2×10^5) were injected into the right hemisphere. After an

additional 2 weeks, the brain with embedded tumors was dissected and subjected to imaging mass spectrometry with Mass Microscope (Shimadzu, Kyoto, Japan). More detailed version of methods and additional methodology are included in Supplementary Methods.

Results

EGFR promotes cell surface expression of xCT in glioma cells

To investigate the mechanism underlying the regulation of xCT expression in CD44s-expressing cancer cells, we studied human glioma cell lines that express CD44s but not CD44v (Fig. 1A). Examination of xCT expression in these cells revealed that T98G showed the highest level of such expression and that U87MG and Becker showed the lowest levels (Fig. 1B). To identify cell surface proteins that show an expression profile similar to that of xCT in T98G cells (xCT^{high}) as well as U87MG and Becker cells (xCT^{low}), we performed flow cytometric analysis of various proteins that had previously been found to be overexpressed in malignant glioma cells (21–29). Among the examined cell surface molecules, the expression profile of EGFR was found to be similar to that of xCT in these glioma cells (Fig. 1C). To examine further the relevance of EGFR to xCT expression in glioma cells, we depleted EGFR in T98G cells by RNA interference (RNAi). Knockdown of EGFR reduced the abundance of xCT at the cell surface (Fig. 1D). Furthermore, expression of a siRNA-resistant EGFR construct prevented the down-regulation of surface xCT expression induced by knockdown of endogenous EGFR (Fig. 1E). Together, these results suggested that the xCT expression is associated with that of EGFR in these xCT^{high} glioma cells. We next investigated MGG18 and GB2 primary human glioblastoma cells (19, 20). Flow cytometry showed that depletion of EGFR by RNAi reduced the surface xCT expression in both MGG18 and GB2 cells (Fig. 1F), suggesting that EGFR expression is also associated with the surface xCT expression in patient-derived glioblastoma cells.

The expression level of EGFR is correlated with that of xCT in human gliomas

Given that EGFR gene is often amplified and overexpressed in glioma cells (30, 31), we next examined whether the expression level of EGFR is related to that of xCT in clinical glioma specimens. Immunostaining of 140 such specimens revealed that the level of xCT expression was significantly higher in EGFR-positive samples than in EGFR-negative samples, whereas it was similar in CD44-positive and CD44-negative samples (Fig. 2A). Furthermore, the expression level of EGFR in the 56 EGFR-positive gliomas was significantly correlated with that of xCT (Fig. 2B, C). These results suggested that the expression of xCT is associated with that of EGFR, but not with that of CD44, in human gliomas.

EGFR interacts with xCT through its intracellular domain and thereby promotes surface xCT expression

To examine the mechanism underlying regulation of xCT expression by EGFR, we depleted T98G cells of EGFR by RNAi. Knockdown of EGFR reduced the total abundance of xCT (Fig. 3A), suggesting that EGFR might affect the amount of cell surface xCT expression by influencing the overall level of this protein.

Given that EGFR influences cancer cell behavior in both a kinase-dependent and -independent manner (32, 33), we made use of the EGFR tyrosine kinase inhibitor gefitinib. Whereas 1 or 2 μM gefitinib blocked EGF-induced activation of EGFR in T98G cells (Fig. 3B), it had no effect on the total abundance (Fig. 3C) or cell surface expression (Supplementary Fig. S1A) of xCT, suggesting that EGFR promotes xCT expression in a manner independent of its kinase activity. Furthermore, the abundance of xCT mRNA did not differ between control and EGFR-depleted T98G cells (Fig. 3D), indicating that the effect of EGFR on xCT protein level is independent of transcriptional control of the xCT gene. Given that the localization of cell surface xCT is associated with an increase in its protein stability (6), we next examined whether EGFR knockdown might reduce the stability of xCT protein. Treatment of cells with the protein synthesis inhibitor cycloheximide revealed that the level of xCT declined at a faster rate in EGFR-depleted cells than in control cells (Fig. 3E). Together, these observations suggested that EGFR increases the stability of xCT protein and thereby enhances the cell surface xCT expression in glioma cells.

Given that the physical interaction of CD44v with xCT promotes the cell surface expression and function of xCT through protein stabilization (6), we next investigated whether EGFR physically interacts with xCT in EGFR-expressing glioma cells. Immunoprecipitation analysis revealed that EGFR indeed interacts with xCT in T98G cells (Fig. 3F). Immunofluorescence staining also showed extensive colocalization of EGFR and xCT in these cells (Supplementary Fig. S1B). We further examined the interaction between EGFR and xCT in T98G cells with the use of a proximity ligation assay (PLA), which allows direct observation of endogenous protein-protein interaction (34). In situ PLA signals (red dots), which reflect protein-protein interaction, were detected with target antibodies to EGFR and to xCT (Fig. 3G), providing further evidence that endogenous EGFR interacts with endogenous xCT in glioma cells.

We next examined whether CD44 expression is indeed dispensable for EGFR-mediated promotion of surface xCT expression in glioma cells. Flow cytometry revealed that EGFR knockdown markedly reduced the surface xCT expression not only in T98G cells expressing a control shRNA but also in those expressing a CD44 shRNA (Supp Fig S1C,D), suggesting that EGFR-dependent promotion of surface xCT expression is independent of CD44 expression status in these cells. Consistent with these results, co-immunoprecipitation analysis showed that the EGFR-xCT complex precipitated from T98G cells (Supplementary Fig. S1E) or from patient-derived MGG18 or GB2 cells (Supplementary Fig. S1F) was devoid of CD44. Both MGG18 and GB2 cells also manifested endogenous EGFR-xCT interaction in the in situ PLA assay (Supplementary Fig. S1G). These results thus suggested that physical interaction with EGFR promotes the surface xCT expression.

To identify the domain of EGFR that mediates xCT interaction, we performed immunoprecipitation analysis with HEK293T cells expressing various EGFR deletion mutants (Fig. 3H). Wild-type (WT) EGFR as well as the mutants EGFRvIII and ΔN-term were found to interact with xCT, whereas the mutant ΔC-term, which lacks most of the intracellular domain, did not (Fig. 3H), indicating that the intracellular domain of EGFR is required for xCT interaction. Forced expression of the ΔN-term mutant, but not that of ΔC-term, also increased surface xCT expression in EGFR-depleted T98G glioma cells (Fig. 3I),

suggesting that the intracellular domain of EGFR (residues 685–1186) is essential for the EGFR-xCT interaction that underlies the promotion of surface xCT expression.

We next examined the region of xCT responsible for the interaction with EGFR. xCT contains 12 transmembrane domains as well as NH_2- and COOH-terminal cytoplasmic tails (Fig. 3J). In addition to full-length xCT, deletion mutants lacking the NH_2-terminal (xCT-Δ1-44) or COOH-terminal (xCT- Δ471-501) cytoplasmic tails were found to interact with EGFR in transfected HEK293T cells (Fig. 3J), suggesting that the central portion of xCT containing the 12 transmembrane domains (amino acids 45–470) is sufficient for interaction with EGFR. Together, our data thus suggested that the intracellular domain of EGFR interacts with the central portion of xCT and thereby promotes surface xCT expression.

Surface xCT regulates redox status and thereby supports glioma cell viability

Given that an increase in the amount of surface xCT enhances cystine uptake (6), we next examined whether EGFR expression might promote cystine uptake in glioma cells with the use of U87MG cells stably overexpressing EGFR (U87MG-EGFR cells). The level of surface xCT expression in U87MG-EGFR cells was increased compared with that in the parental U87MG cells, whereas the amount of xCT mRNA did not differ between the two cell lines (Fig. 4A, Supplementary Fig. S2A). The extent of L-cystine uptake (Fig. 4B, Supplementary Table S1) as well as the intracellular level of cysteine (Supplementary Fig. S2B) in U87MG-EGFR cells were significantly increased compared with those in U87MG cells, suggesting that forced expression of EGFR might promote cystine uptake and thereby increase intracellular cysteine abundance through enhancement of surface xCT expression. Given that the availability of cysteine is rate-limiting for GSH synthesis, we also measured the levels of GSH and total glutathione in these cells. The amounts of both GSH and total glutathione (GSH + the disulfide-linked dimer GSSG) were significantly increased in U87MG-EGFR cells compared with parental U87MG cells (Fig. 4C). Conversely, depletion of EGFR in T98G cells significantly reduced the intracellular abundance of GSH (Supplementary Fig. S2C). Furthermore, imaging mass spectrometry revealed that brain tumors formed by U87MG-EGFR cells in mice showed markedly higher GSH levels than did those formed by U87MG cells (Fig. 4D), suggesting that the up-regulation of surface xCT expression by EGFR results in the increased GSH synthesis in glioma cells in vivo. Together, our observations thus indicated that EGFR up-regulates the surface xCT expression and thereby increases cystine uptake and GSH synthesis in glioma cells.

To determine whether the up-regulation of xCT-dependent cystine transport by EGFR plays a role in maintenance of the redox status in glioma cells, we examined the effects of sulfasalazine, a specific inhibitor of xCT. The viability of xCT^{high} glioma cells (T98G and U87MG-EGFR) was highly sensitive to sulfasalazine, whereas that of xCT^{low} glioma cells (U87MG and Becker) was less so (Fig. 4E), suggesting that $EGFR^{high}$ glioma cells depend on xCT-mediated cystine transport for their survival. To investigate further the role of xCT-dependent cystine transport in $EGFR^{high}$ cancer cells, we examined whether xCT might regulate the intracellular ROS level in these cells. Sulfasalazine increased the intracellular ROS level in $EGFR^{high}/xCT^{high}$ glioma cells (U87MG-EGFR and T98G) in a manner sensitive to the presence of exogenous antioxidants such as Trolox and *N*-acetylcysteine

(NAC) (Fig. 4F). In contrast, sulfasalazine failed to increase the intracellular ROS level in $EGFR^{low}/xCT^{low}$ cells (U87MG and Becker) (Supplementary Fig. S2D). These results suggested that xCT-dependent cystine transport regulates redox status in $EGFR^{high}/xCT^{high}$ glioma cells but not in $EGFR^{low}/xCT^{low}$ cells.

We next examined whether the disruption of redox status by sulfasalazine contributes to the cytotoxic effect of this drug on $EGFR^{high}/xCT^{high}$ glioma cells. The antioxidants Trolox and NAC, but not glutamate, which is released by xCT in exchange for cystine, prevented the decrease in cell viability induced by sulfasalazine in both U87MG-EGFR and T98G cells (Fig. 4G), implicating disruption of redox status due to cysteine depletion in sulfasalazine-induced suppression of cell survival in $EGFR^{high}/xCT^{high}$ glioma cells. Depletion of xCT by RNAi also suppressed the viability of U87MG-EGFR cells without affecting that of U87MG cells (Supplementary Fig. S2E), suggesting that EGFR expression is associated with xCT dependency in glioma cells.

We examined whether sulfasalazine might affect EGFR signaling in glioma cells. However, we found that sulfasalazine had no effect on the EGF-induced EGFR phosphorylation of EGFR or its downstream targets ERK (extracellular signal–regulated kinase) and AKT (Supplementary Fig. S2F), suggesting that sulfasalazine reduces the viability of $EGFR^{high}/xCT^{high}$ glioma cells without affecting EGFR signaling.

Given that sulfasalazine reduced cell survival of $EGFR^{high}/xCT^{high}$ glioma cells, we next examined whether the depletion of EGFR which regulates surface xCT expression reduces the cell viability of these cells. Similar to sulfasalazine treatment, RNAi-mediated EGFR depletion significantly reduced cell viability of T98G cells, whereas forced expression of xCT markedly recovered the viability of EGFR-depleted T98G cells (Fig. 4H), suggesting that $EGFR^{high}/xCT^{high}$ glioma cells depend on the EGFR-promoted activity of system xc(−) for their survival.

We also examined the impact of sulfasalazine on the subcutaneous tumors formed by $EGFR^{low}/xCT^{low}$ (U87MG) or $EGFR^{high}/xCT^{high}$ (U87MG-EGFR) cells in nude mice. Administration of sulfasalazine attenuated the growth of tumors formed by U87MG-EGFR cells but not that of those formed by U87MG cells (Fig. 4I), suggesting that xCT plays a role in tumor growth in $EGFR^{high}/xCT^{high}$ glioma cells but not in $EGFR^{low}/xCT^{low}$ cells. Given that the chemotherapeutic drug cisplatin exerts its anticancer effects in part through ROS generation in cancer cells (35), we next examined whether sulfasalazine might enhance the antitumor effect of cisplatin. Administration of sulfasalazine was indeed found to enhance the antitumor effect of cisplatin on tumor xenografts formed by U87MG-EGFR cells (Fig. 4I), suggesting that the sulfasalazine-induced attenuation of ROS defense sensitizes $EGFR^{high}/xCT^{high}$ glioma cells to ROS-inducing anticancer agents. Together, these observations indicated that xCT-dependent cystine transport contributes to the maintenance of redox status and thereby promotes cell survival and tumorigenesis in $EGFR^{high}/xCT^{high}$ glioma cells but not in $EGFR^{low}/xCT^{low}$ cells.

Inhibition of system xc(−) suppresses EGFR-expressing glioma cell invasion

Given that extracellular glutamate has been shown to enhance cell motility (16), we next examined the possible role of glutamate release through system xc(−) in glioma cell migration. Glutamate release was found to be markedly increased in U87MG-EGFR cells compared with U87MG cells (Fig. 5A). Furthermore, knockdown of xCT or EGFR in U87MG-EGFR cells reduced the level of glutamate release to that apparent in parental U87MG cells (Fig. 5A). In contrast, gefitinib did not affect the level of glutamate release (Fig. 5A), suggesting that EGFR kinase activity is dispensable for the enhancement of xCT-mediated glutamate release by EGFR. U87MG cells stably expressing the EGFRvIII mutant (U87MG-EGFRvIII cells) also showed increased levels of surface xCT expression (Supplementary Fig. S3A) and glutamate release (Supplementary Fig. S3B) compared with parental U87MG cells. Furthermore, EGFR knockdown reduced the extent of glutamate release in the patient-derived MGG18 and GB2 cells (Fig. 5B). Together, these results suggested that glutamate release mediated by xCT in glioma cells is enhanced by EGFR or EGFRvIII expression in a manner independent of EGFR kinase activity.

Given that glutamate is thought to promote cell migration in an autocrine manner (16), we examined whether the inhibition of glutamate release might suppress the migration of glioma cells. An in vitro scratch assay revealed that sulfasalazine inhibited the migration of T98G cells and that this inhibition was attenuated by the addition of glutamate (Fig. 5C), suggesting that released glutamate promotes glioma cell migration in an autocrine manner. We next examined whether xCT-dependent glutamate release plays a role in the promotion of glioma cell migration by various chemoattractants (16). Sulfasalazine significantly inhibited the stimulatory effects of serum, EGF, Amphiregulin, and TGF-α on U87MG-EGFR cell migration, and this inhibition was prevented by the addition of glutamate (Fig. 5D). We also found that sulfasalazine significantly inhibited extracellular matrix invasion by the patient-derived MGG18 and GB2 glioblastoma cells and that this inhibition was prevented by glutamate (Fig. 5E). These results suggested that xCT-dependent glutamate release promotes migration and invasion by glioma cells.

To examine the functional relevance of xCT to glioma cell invasion in the brain, we employed organotypic brain slice culture system (Fig. 5F). EGF promoted the invasion of U87MG-EGFR cells in this model in a manner sensitive to inhibition by the xCT inhibitor sulfasalazine (Fig. 5G, H).

Finally, to evaluate the potential of xCT as a therapeutic target for $EGFR^{high}$ glioma, we examined whether RNAi-mediated depletion of xCT in U87MG-EGFR cells might affect the survival of mice with orthotopic tumors formed by these cells. Stable depletion of xCT prolonged survival compared with that observed in mice implanted with control U87MG-EGFR cells (Fig. 5I). Together, these observations indicated that xCT plays a key role in the malignant behavior of glioma and that system xc(−) is therefore a promising target for cancer therapy, especially for the treatment of $EGFR^{high}$ glioma.

Discussion

Conventional cancer treatments including chemotherapy and radiation therapy induce the generation of cytotoxic ROS in cancer cells. Strategies to abrogate ROS defense in cancer cells might therefore be expected to provide a basis for the development of new and efficient cancer therapies (36–38). The expression of xCT is thought to be related to malignant potential in glioma (8), and a recent study showed that xCT expression correlates with tumor growth, glutamate-induced seizures, and poor prognosis in patients with malignant glioma (39). We have now shown that EGFR interacts through its intracellular domain with, and thereby promotes the surface xCT expression, leading to an increase in cystine uptake and GSH synthesis in glioma cells that do not express CD44v. Furthermore, the vIII mutant of EGFR also interacted with and increased the surface xCT expression, suggesting that the expression level of EGFR, including both WT and mutant forms, is a determinant of the activity of system xc(−) in glioma cells. However, the EGFR kinase inhibitor gefitinib had no effect on the surface xCT expression in $EGFR^{high}$ glioma cells. Together, our results thus suggest that the cytoplasmic domain of EGFR interacts with the central portion of xCT and thereby increases the surface xCT expression in a kinase-independent manner.

CD44 was previously shown to interact with EGFR and to influence EGFR signaling (40), and CD44 and EGFR were found to be present in the same protein complex and to cooperatively promote cancer cell invasion (41). However, in the present study with glioma cells, we found that CD44 did not interact with EGFR and that the regulation of xCT expression by EGFR was not affected by CD44. Given that the pattern of CD44 isoform expression differs among cancer types, the molecular interaction of CD44 with EGFR might be differentially regulated in a manner dependent on cell type.

Inhibition of xCT-dependent cystine transport, which is potentiated by CD44v, induces cell death selectively in CD44v-expressing stemlike tumor cells (42). Consistent with this previous observation, we found that glioma cells engineered to stably express EGFR were more sensitive to sulfasalazine compared with the parental cells, suggesting that $EGFR^{high}$ glioma cells that also express xCT at a high level at the cell surface depend on system xc(−) for regulation of intracellular redox status. Given that EGFR activation results in the generation of ROS that act as a second messenger for physiological cellular signaling (43–45), $EGFR^{high}$ glioma cells might depend on xCT-mediated ROS defense to avoid the harmful effects of ROS accumulation. Together, these findings suggest that enhancement of GSH synthesis by EGFR or CD44v may reprogram the antioxidant system of cancer cells, and that EGFR- or CD44v-expressing cancer cells, in which GSH plays a central role in the regulation of redox status, are potential targets of xCT inhibitors.

Recently, system xc(−) in malignant glioma cells was shown to play a key role in the development of a glutamate-rich microenvironment that promotes neurodegeneration, brain edema, and glioma invasion (13, 46). We have now shown that $EGFR^{high}$ or $EGFRvIII^{high}$ glioma cells that also express xCT at a high level at the cell surface release relatively large amounts of glutamate through system xc(−), suggesting that EGFR-xCT interaction in glioma cells promotes the release of glutamate, which then contributes to both cell-autonomous and chemotactic migration of $EGFR^{high}$ glioma cells.

In conclusion, our present data provide evidence that the association of EGFR with xCT enhances ROS defense in and matrix invasion by glioma cells. Given that aggressive glioma cells often generate a glutamate-rich microenvironment, the EGFR-xCT axis might be a promising therapeutic target for $EGFR^{high}$ or $EGFRvIII^{high}$ glioma.

Supplementary Material

Refer to Web version on PubMed Central for supplementary material.

Acknowledgments

Financial support: This work was supported by grants (to H.S.) from, as well as in part by the Project for Development of Innovative Research on Cancer Therapeutics (P-Direct) (to O.N.) of, the Ministry of Education, Culture, Sports, Science, and Technology of Japan.

We thank all members of the Saya lab for technical assistance, material support and helpful suggestion as well as M. Sato and K. Arai for help in preparation of the manuscript.

References

1. Al-Zhoughbi W, Huang J, Paramasivan GS, Till H, Pichler M, Guertl-Lackner B, et al. Tumor macroenvironment and metabolism. Semin Oncol. 2014; 41:281–95. [PubMed: 24787299]
2. Cantor JR, Sabatini DM. Cancer cell metabolism: one hallmark, many faces. Cancer Discov. 2012; 2:881–98. [PubMed: 23009760]
3. Zhang W, Trachootham D, Liu J, Chen G, Pelicano H, Garcia-Prieto C, et al. Stromal control of cystine metabolism promotes cancer cell survival in chronic lymphocytic leukaemia. Nat Cell Biol. 2012; 14:276–86. [PubMed: 22344033]
4. Ganapathy V, Thangaraju M, Prasad PD. Nutrient transporters in cancer: relevance to Warburg hypothesis and beyond. Pharmacol Ther. 2009; 121:29–40. [PubMed: 18992769]
5. Sato H, Shiiya A, Kimata M, Maebara K, Tamba M, Sakakura Y, et al. Redox imbalance in cystine/glutamate transporter-deficient mice. J Biol Chem. 2005; 280:37423–9. [PubMed: 16144837]
6. Ishimoto T, Nagano O, Yae T, Tamada M, Motohara T, Oshima H, et al. CD44 variant regulates redox status in cancer cells by stabilizing the xCT subunit of system xc(–) and thereby promotes tumor growth. Cancer Cell. 2011; 19:387–400. [PubMed: 21397861]
7. Huang Y, Dai Z, Barbacioru C, Sadée W. Cystine-glutamate transporter SLC7A11 in cancer chemosensitivity and chemoresistance. Cancer Res. 2005; 65:7446–54. [PubMed: 16103098]
8. Lo M, Wang YZ, Gout PW. The x(c)- cystine/glutamate antiporter: a potential target for therapy of cancer and other diseases. J Cell Physiol. 2008; 215:593–602. [PubMed: 18181196]
9. Yae T, Tsuchihashi K, Ishimoto T, Motohara T, Yoshikawa M, Yoshida GJ, et al. Alternative splicing of CD44 mRNA by ESRP1 enhances lung colonization of metastatic cancer cell. Nat Commun. 2012; 3:883. [PubMed: 22673910]
10. Nagano O, Okazaki S, Saya H. Redox regulation in stem-like cancer cells by CD44 variant isoforms. Oncogene. 2013; 32:5191–8. [PubMed: 23334333]
11. Ranuncolo SM, Ladeda V, Specterman S, Varela M, Lastiri J, Morandi A, et al. CD44 expression in human gliomas. J Surg Oncol. 2002; 79:30–5. [PubMed: 11754374]
12. Brown RL, Reinke LM, Damerow MS, Perez D, Chodosh LA, Yang J, et al. CD44 splice isoform switching in human and mouse epithelium is essential for epithelial-mesenchymal transition and breast cancer progression. J Clin Invest. 2012; 121:1064–74. [PubMed: 21393860]
13. de Groot J, Sontheimer H. Glutamate and the biology of gliomas. Glia. 2011; 59:1181–9. [PubMed: 21192095]
14. Timmerman LA, Holton T, Yuneva M, Louie RJ, Padró M, Daemen A, et al. Glutamine sensitivity analysis identifies the xCT antiporter as a common triple-negative breast tumor therapeutic target. Cancer Cell. 2013; 24:450–65. [PubMed: 24094812]

15. Takano T, Lin JH, Arcuino G, Gao Q, Yang J, Nedergaard M. Glutamate release promotes growth of malignant gliomas. Nat Med. 2001; 7:1010–5. [PubMed: 11533703]
16. Lyons SA, Chung WJ, Weaver AK, Ogunrinu T, Sontheimer H. Autocrine glutamate signaling promotes glioma cell invasion. Cancer Res. 2007; 67:9463–71. [PubMed: 17909056]
17. Ye ZC, Sontheimer H. Glioma cells release excitotoxic concentrations of glutamate. Cancer Res. 1999; 59:4383–91. [PubMed: 10485487]
18. Savaskan NE, Heckel A, Hahnen E, Engelhorn T, Doerfler A, Ganslandt O, et al. Small interfering RNA-mediated xCT silencing in gliomas inhibits neurodegeneration and alleviates brain edema. Nat Med. 2008; 14:629–32. [PubMed: 18469825]
19. Wakimoto H, Mohapatra G, Kanai R, Curry WT Jr, Yip S, Nitta M, et al. Maintenance of primary tumor phenotype and genotype in glioblastoma stem cells. Neuro Oncol. 2012; 14:132–44. [PubMed: 22067563]
20. Koyama-Nasu R, Haruta R, Nasu-Nishimura Y, Taniue K, Katou Y, Shirahige K, et al. The pleiotrophin-ALK axis is required for tumorigenicity of glioblastoma stem cells. Oncogene. 2014; 33:2236–44. [PubMed: 23686309]
21. Gammeltoft S, Ballotti R, Kowalski A, Westermark B, Van Obberghen E. Expression of two types of receptor for insulin-like growth factors in human malignant glioma. Cancer Res. 1988; 48:1233–7. [PubMed: 2963688]
22. Ehtesham M, Winston JA, Kabos P, Thompson RC. CXCR4 expression mediates glioma cell invasiveness. Oncogene. 2006; 25:2801–6. [PubMed: 16407848]
23. Puputti M, Tynninen O, Sihto H, Blom T, Mäenpää H, Isola J, et al. Amplification of KIT, PDGFRA, VEGFR2, and EGFR in gliomas. Mol Cancer Res. 2006; 4:927–34. [PubMed: 17189383]
24. Li JL, Sainson RC, Shi W, Leek R, Harrington LS, Preusser M, et al. Delta-like 4 Notch ligand regulates tumor angiogenesis, improves tumor vascular function, and promotes tumor growth in vivo. Cancer Res. 2007; 67:11244–53. [PubMed: 18056450]
25. Brescia P, Richichi C, Pelicci G. Current strategies for identification of glioma stem cells: adequate or unsatisfactory? J Oncol. 2012; 2012:376894. [PubMed: 22685459]
26. Hamerlik P, Lathia JD, Rasmussen R, Wu Q, Bartkova J, Lee M, et al. Autocrine VEGF-VEGFR2-Neuropilin-1 signaling promotes glioma stem-like cell viability and tumor growth. J Exp Med. 2012; 209:507–20. [PubMed: 22393126]
27. Dahlrot RH, Hermansen SK, Hansen S, Kristensen BW. What is the clinical value of cancer stem cell markers in gliomas? Int J Clin Exp Pathol. 2013; 6:334–48. [PubMed: 23412423]
28. Mao XG, Xue XY, Wang L, Zhang X, Yan M, Tu YY, et al. CDH5 is specifically activated in glioblastoma stemlike cells and contributes to vasculogenic mimicry induced by hypoxia. Neuro Oncol. 2013; 15:865–79. [PubMed: 23645533]
29. Pietras A, Katz AM, Ekström EJ, Wee B, Halliday JJ, Pitter KL, et al. Osteopontin-CD44 signaling in the glioma perivascular niche enhances cancer stem cell phenotypes and promotes aggressive tumor growth. Cell Stem Cell. 2014; 14:357–69. [PubMed: 24607407]
30. Hatanpaa KJ, Burma S, Zhao D, Habib AA. Epidermal growth factor receptor in glioma: signal transduction, neuropathology, imaging, and radioresistance. Neoplasia. 2010; 12:675–84. [PubMed: 20824044]
31. Taylor TE, Furnari FB, Cavenee WK. Targeting EGFR for treatment of glioblastoma: molecular basis to overcome resistance. Curr Cancer Drug Targets. 2012; 12:197–209. [PubMed: 22268382]
32. Weihua Z, Tsan R, Huang WC, Wu Q, Chiu CH, Fidler IJ, et al. Survival of cancer cells is maintained by EGFR independent of its kinase activity. Cancer Cell. 2008; 13:385–93. [PubMed: 18455122]
33. Fan QW, Cheng CK, Gustafson WC, Charron E, Zipper P, Wong RA, et al. EGFR phosphorylates tumor-derived EGFRvIII driving STAT3/5 and progression in glioblastoma. Cancer Cell. 2013; 24:438–49. [PubMed: 24135280]
34. Söderberg O, Gullberg M, Jarvius M, Ridderstråle K, Leuchowius KJ, Jarvius J, et al. Direct observation of individual endogenous protein complexes in situ by proximity ligation. Nat Methods. 2006; 3:995–1000. [PubMed: 17072308]

35. Conklin KA. Chemotherapy-associated oxidative stress: impact on chemotherapeutic effectiveness. Integr Cancer Ther. 2004; 3:294–300. [PubMed: 15523100]
36. Trachootham D, Alexandre J, Huang P. Targeting cancer cells by ROS-mediated mechanisms: a radical therapeutic approach? Nat Rev Drug Discov. 2009; 8:579–91. [PubMed: 19478820]
37. Gorrini C, Harris IS, Mak TW. Modulation of oxidative stress as an anticancer strategy. Nat Rev Drug Discov. 2013; 12:931–47. [PubMed: 24287781]
38. Nogueira V, Hay N. Molecular pathways: reactive oxygen species homeostasis in cancer cells and implications for cancer therapy. Clin Cancer Res. 2013; 19:4309–14. [PubMed: 23719265]
39. Robert SM, Buckingham SC, Campbell SL, Robel S, Holt KT, Ogunrinu-Babarinde T, et al. SLC7A11 expression is associated with seizures and predicts poor survival in patients with malignant glioma. Sci Transl Med. 2015; 7:289ra86.
40. Perez A, Neskey DM, Wen J, Pereira L, Reategui EP, Goodwin WJ, et al. CD44 interacts with EGFR and promotes head and neck squamous cell carcinoma initiation and progression. Oral Oncol. 2013; 49:306–13. [PubMed: 23265944]
41. Grass GD, Tolliver LB, Bratoeva M, Toole BP. CD147, CD44, and the epidermal growth factor receptor (EGFR) signaling pathway cooperate to regulate breast epithelial cell invasiveness. J Biol Chem. 2013; 288:26089–104. [PubMed: 23888049]
42. Yoshikawa M, Tsuchihashi K, Ishimoto T, Yae T, Motohara T, Sugihara E, et al. xCT inhibition depletes CD44v-expressing tumor cells that are resistant to EGFR-targeted therapy in head and neck squamous cell carcinoma. Cancer Res. 2013; 73:1855–66. [PubMed: 23319806]
43. Miller EW, Tulyathan O, Isacoff EY, Chang CJ. Molecular imaging of hydrogen peroxide produced for cell signaling. Nat Chem Biol. 2007; 3:263–7. [PubMed: 17401379]
44. Paulsen CE, Truong TH, Garcia FJ, Homann A, Gupta V, Leonard SE, et al. Peroxide-dependent sulfenylation of the EGFR catalytic site enhances kinase activity. Nat Chem Biol. 2011; 8:57–64. [PubMed: 22158416]
45. Truong TH, Carroll KS. Redox regulation of epidermal growth factor receptor signaling through cysteine oxidation. Biochemistry. 2012; 51:9954–65. [PubMed: 23186290]
46. Savaskan NE, Eyüpoglu IY. xCT modulation in gliomas: relevance to energy metabolism and tumor microenvironment normalization. Ann Anat. 2010; 192:309–13. [PubMed: 20801625]

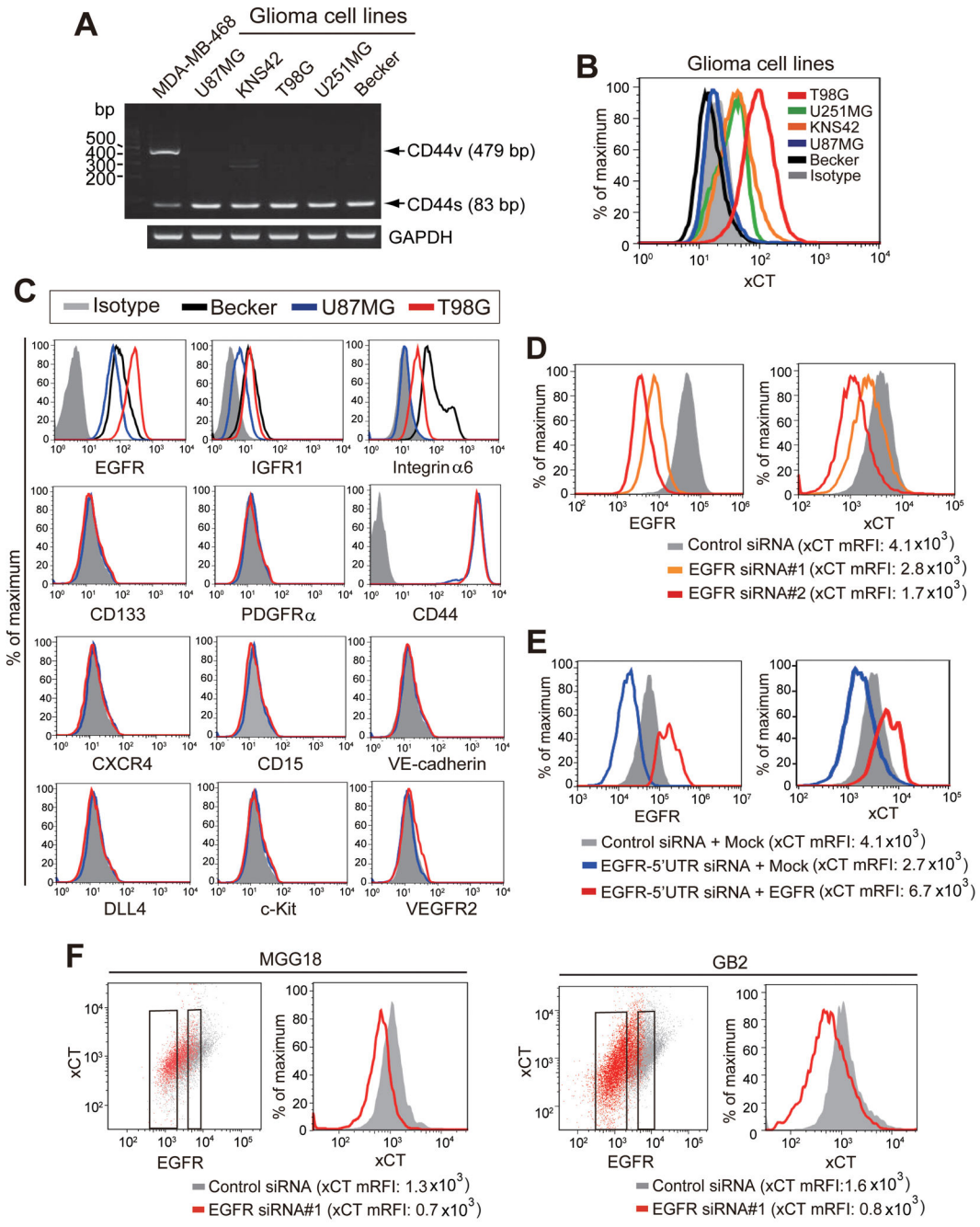

Figure 1. EGFR promotes surface xCT expression in glioma cells

(**A**) Reverse transcription (RT) and PCR analysis with primers targeted to exons 5 and 16 of the human CD44 gene as well as to the human glyceraldehyde-3-phosphate dehydrogenase (GAPDH) gene. The breast cancer cell line MDA-MB-468 was examined as a positive control for CD44v expression.

(**B**) Flow cytometric analysis of surface xCT expression in the indicated cell lines. Staining of T98G cells with an isotype control antibody is also shown.

(**C**) Flow cytometric analysis of surface expression of the indicated proteins in xCT^{low} (U87MG and Becker for EGFR, IGFR1, and integrin α6) and xCT^{high} (T98G) cells.
(**D**) Flow cytometric analysis of surface expression of EGFR and xCT in T98G cells transfected with control or EGFR siRNAs. mRFI, mean value for relative fluorescence intensity.
(**E**) Flow cytometric analysis of surface expression of EGFR and xCT in T98G cells transfected with a control siRNA or an siRNA targeted to the 5′ untranslated region (5′UTR) of EGFR mRNA as well as with an expression vector for EGFR lacking the 5′UTR or with the corresponding empty vector (Mock).
(**F**) Flow cytometric analysis of surface expression of EGFR and xCT in MGG18 and GB2 cells transfected with control or EGFR siRNAs.

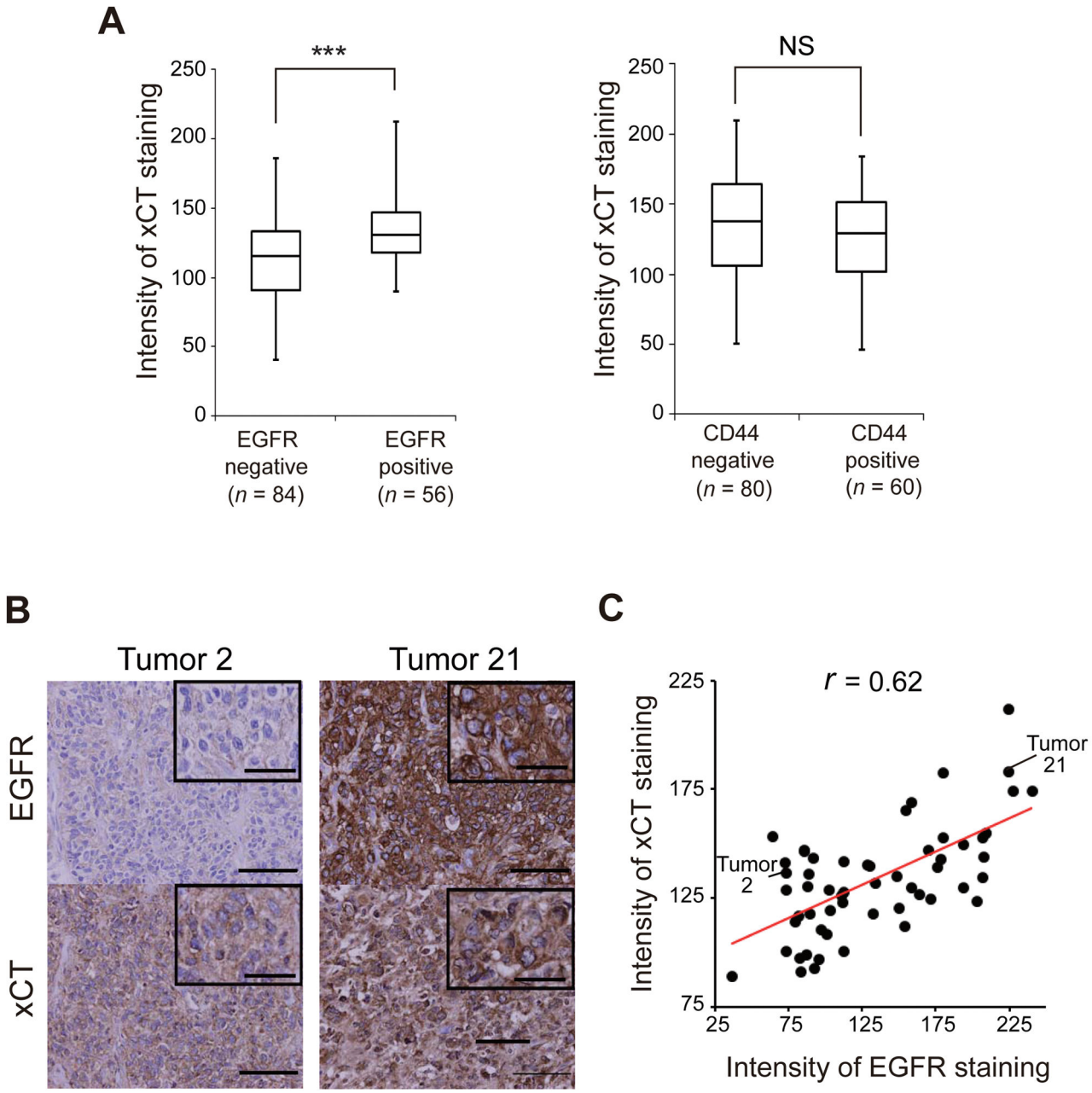

Figure 2. Expression of EGFR is correlated with that of xCT in human gliomas

(**A**) Box-and-whisker plots of xCT immunostaining intensity for glioma specimens that were negative ($n = 84$) or positive ($n = 56$) for EGFR staining (left panel) or negative ($n = 80$) or positive ($n = 60$) for CD44 staining (right panel). ***$p < 0.001$; NS, not significant (Student's t test).

(**B**) Immunohistochemical analysis of EGFR and xCT in human glioma specimens. Tumor 21 shows more intense staining for both EGFR and xCT compared with tumor 2. Scale bars, 100 μm (main panels) or 20 μm (insets).

(**C**) Scatter plot for the intensity of immunostaining for EGFR and xCT in 56 specimens of human EGFR-expressing glioma. Pearson's correlation coefficient is indicated by r.

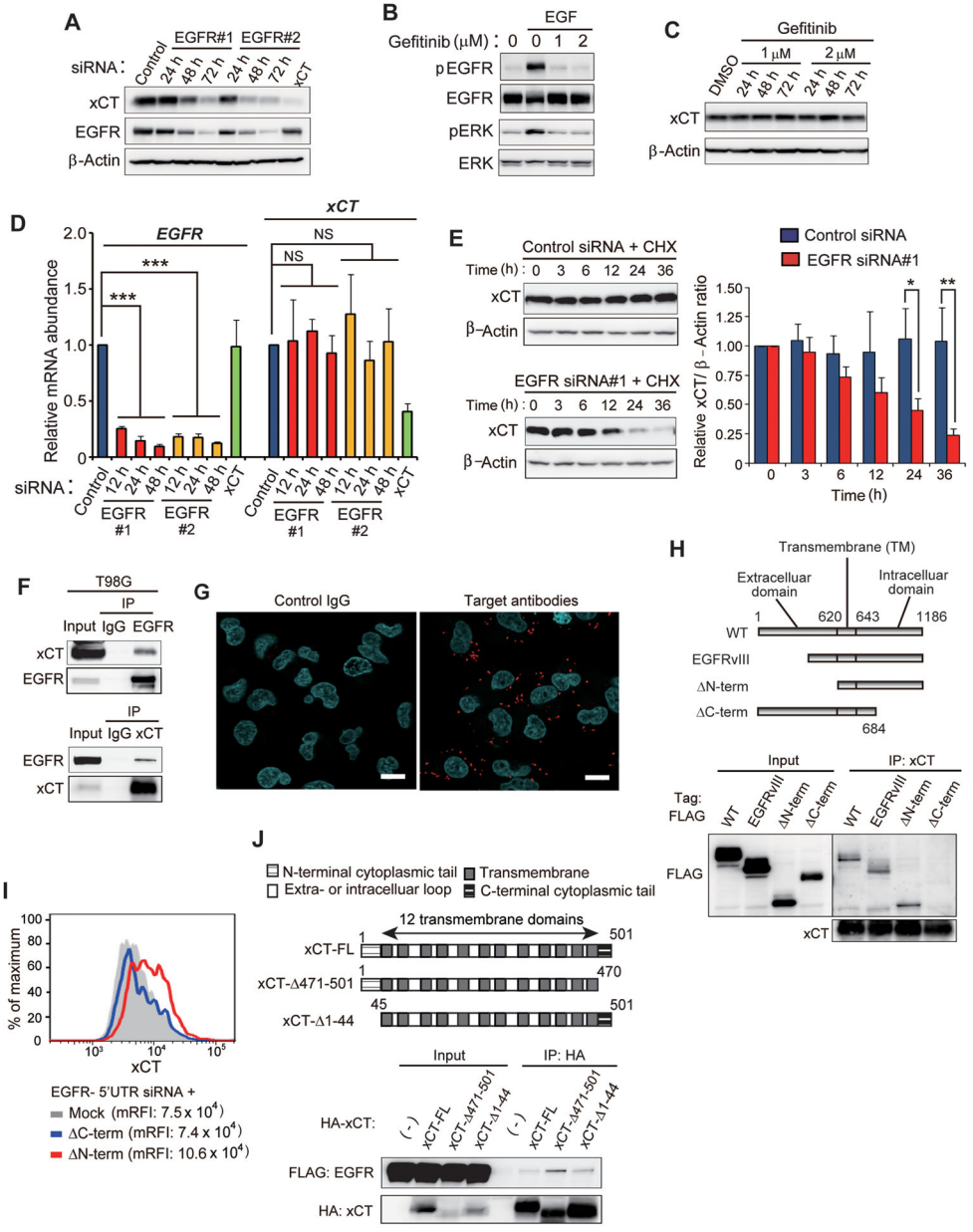

Figure 3. Intracellular domain of EGFR interacts with xCT and thereby promotes its cell surface expression

(**A**) Immunoblot analysis of EGFR, xCT, and β-actin (loading control) in T98G cells transfected with control, EGFR, or xCT siRNAs for 72 h or the indicated times.

(**B**) Immunoblot analysis of total or phosphorylated (p) forms of EGFR and ERK in T98G cells that had been incubated in the absence or presence of EGF (50 ng/ml) or gefitinib (1 or 2 μM) for 30 min.

(**C**) Immunoblot analysis of xCT in T98G cells treated with gefitinib (1 or 2 μM) or dimethyl sulfoxide (DMSO) vehicle) for the indicated times.

(**D**) Quantitative RT-PCR analysis of EGFR and xCT mRNAs in T98G cells transfected with EGFR or xCT siRNAs for the indicated times. ***$p < 0.001$ (Student's *t* test).

(**E**) Immunoblot analysis of xCT in T98G cells transfected with control or EGFR siRNAs for 36 h and then exposed to cycloheximide (CHX, 100 μg/ml) for the indicated times (left panels). The xCT/β-actin band intensity ratios relative to the corresponding value for time zero were determined as means ± SD from three independent experiments (right panel). $*p < 0.05$, $**p < 0.01$ (Student's *t* test).

(**F**) T98G cell lysates were subjected to immunoprecipitation (IP) with antibodies to EGFR or to xCT or with control immunoglobulin G (IgG). The resulting precipitates, as well as 5% of the original cell lysates (Input), were subjected to immunoblot analysis with antibodies to xCT and to EGFR.

(**G**) T98G cells were subjected to a PLA with control IgG (left panel) or antibodies to EGFR and to xCT (right panel). Red dots represent PLA signals. Scale bars, 20 μm.

(**H**) Schematic representation of full-length (WT) and mutant forms of human EGFR. EGFRvIII lacks the amino acid sequence encoded by exons 2 to 7 of the EGFR gene. ΔN-term lacks the extracellular region of EGFR and consists of amino acid residues 621 to 1186, whereas ΔC-term consists of residues 1 to 684 and lacks most of the intracellular domain (upper panel). Lysates of HEK293T cells expressing FLAG-tagged WT or mutant forms of EGFR were subjected to immunoprecipitation with antibodies to xCT, and the resulting precipitates, as well as the original cell lysates (Input), were subjected to immunoblot analysis with antibodies to FLAG or to xCT (lower panel).

(**I**) Flow cytometric analysis of surface xCT expression in T98G cells transfected with an siRNA targeted to the 5′UTR of EGFR mRNA as well as with an expression vector for ΔN-term or ΔC-term mutants of EGFR lacking the 5′UTR sequence or with the corresponding empty vector (Mock).

(**J**) Schematic representation of full-length (FL) and mutant forms of human xCT (upper panel). Lysates of HEK293T cells expressing FLAG-tagged EGFR and hemagglutinin epitope (HA)–tagged full-length or mutant forms of xCT were subjected to immunoprecipitation with antibodies to HA. The resulting precipitates, as well as the original cell lysates (Input), were subjected to immunoblot analysis with antibodies to FLAG and to HA (lower panel).

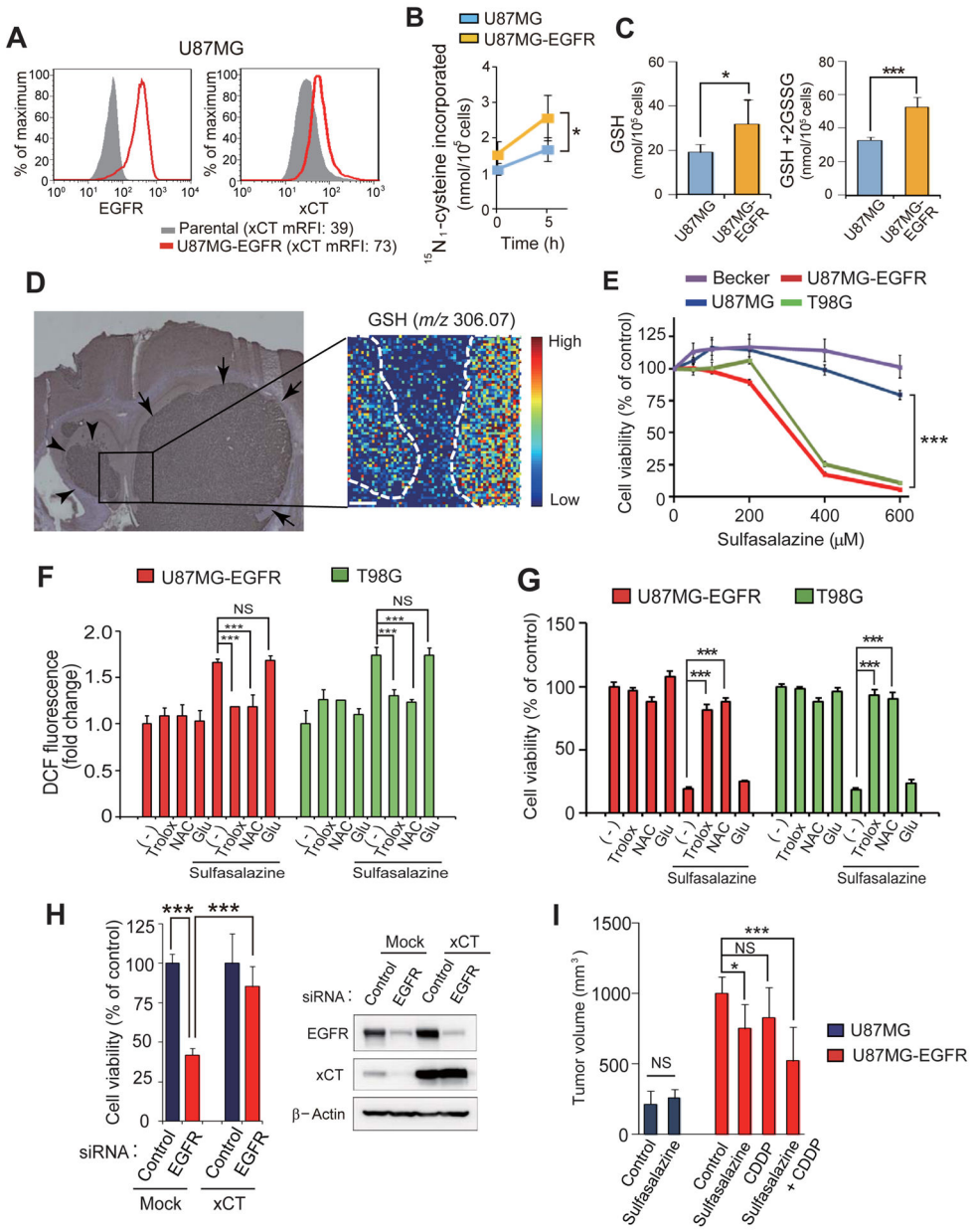

Figure 4. Sulfasalazine disrupts redox status and thereby reduces cell viability in EGFR-expressing glioma cells

(**A**) Flow cytometric analysis of surface expression of EGFR and xCT in U87MG cells stably expressing EGFR (U87MG-EGFR cells) as well as in parental U87MG cells.

(**B**) Measurement of $^{15}N_2$-cystine uptake in U87MG and U87MG-EGFR cells. Data are means ± SD from five separate experiments. *$p < 0.05$ (Student's *t* test). See also Supplementary Table S1 for raw data.

(**C**) Analysis of GSH and total glutathione (GSH + 2GSSG) content in U87MG and U87MG-EGFR cells. Data are means ± SD from five independent experiments.*$p < 0.05$, ***$p < 0.001$ (Student's *t* test).

(**D**) U87MG cells were injected into the left hemisphere and U87MG-EGFR cells were injected into the right hemisphere of NOD/SCID mice. After 2 weeks, the brain with embedded tumors was dissected and serial sections of mouse brain harboring separate tumors formed by U87MG cells (arrowheads) and U87MG-EGFR cells (arrows) were subjected to immunohistochemical staining with antibodies to human vimentin (left panel) as well as to imaging mass spectrometry of GSH (right panel). Scale bar in the right panel, 200 μm. The color scale indicates peak intensity levels at a mass/charge (*m/z*) ratio of 306.07 (GSH).

(**E**) Glioma cell lines were incubated with the indicated concentrations of sulfasalazine for 60 h and then assayed for cell viability. Data are means ± SD from six independent experiments. ***$p < 0.001$ (Student's *t* test).

(**F**) U87MG-EGFR and T98G cells were incubated for 24 h with or without 400 or 600 μM sulfasalazine, respectively and in the absence or presence of 50 μM Trolox, 1 mM NAC, or 250 μM glutamate (Glu), after which the intracellular ROS level was measured on the basis of dichlorofluorescein (DCF) fluorescence. Data are means ± SD from five independent experiments. ***$p < 0.001$ (Student's *t* test).

(**G**) U87MG-EGFR and T98G cells were incubated for 60 h as in (**F**) and then assayed for cell viability. Data are means ± SD from five independent experiments. ***$p < 0.001$ (Student's *t* test).

(**H**) T98G cells transfected with an expression vector for xCT or the corresponding empty vector (Mock) were also transfected with control or EGFR (#1) siRNAs for 72 h and then assayed for cell viability (left panel). Data are means ± SD from five independent experiments. ***$p < 0.001$ (Student's *t* test). Cell lysates were also subjected to immunoblot analysis of EGFR and xCT (right panel).

(**I**) Volume of subcutaneous tumors formed in nude mice by U87MG or U87MG-EGFR cells at 14 days after cell injection and treatment with saline (Control), sulfasalazine (250 mg/kg), cisplatin (CDDP, 2 mg/kg), or sulfasalazine (250 mg/kg) plus cisplatin (2 mg/kg). Data are means ± SD for four or five animals per group. *$p < 0.05$, ***$p < 0.001$ (Student's *t* test).

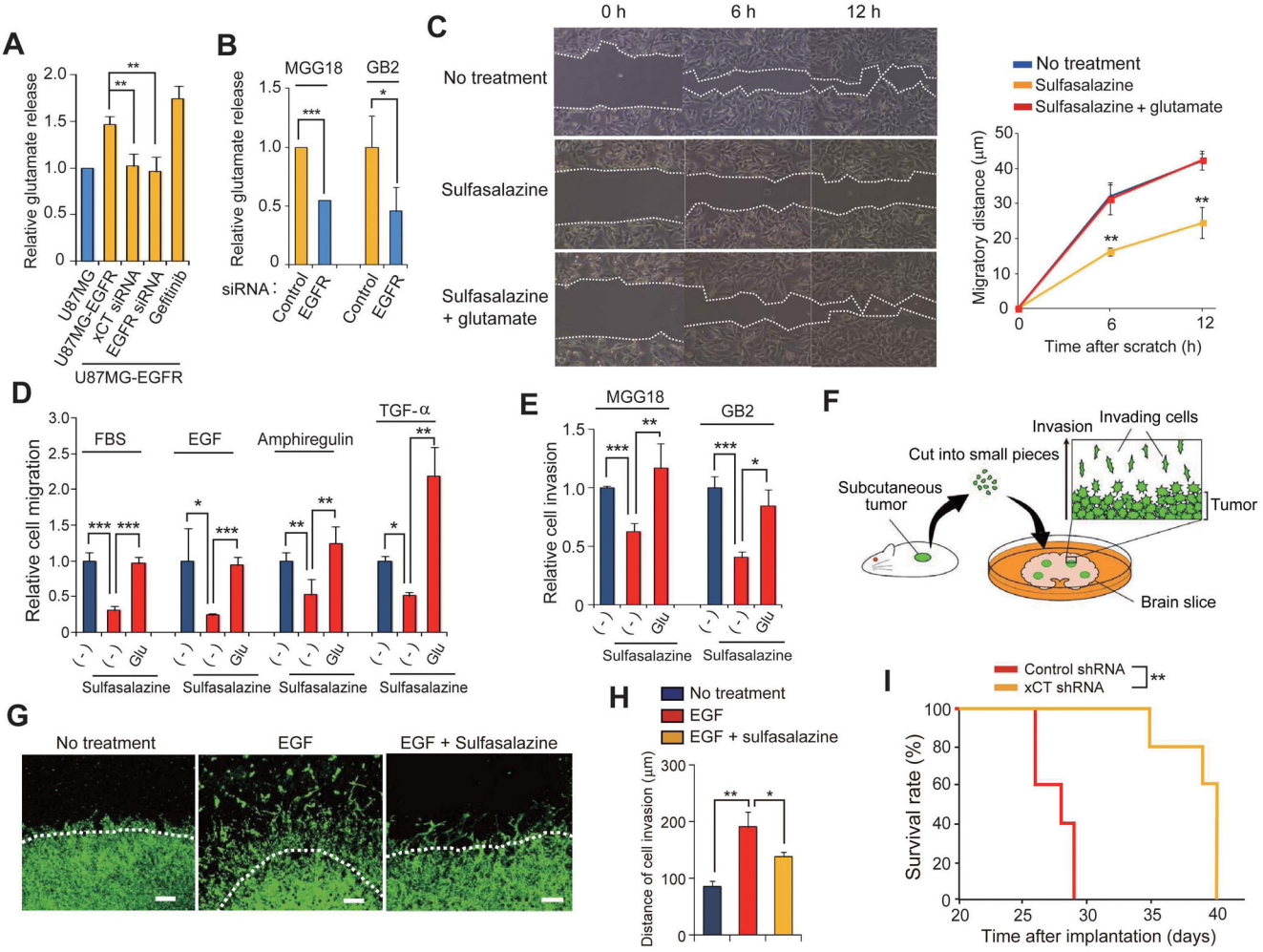

Figure 5. Glutamate release mediated by xCT promotes glioma cell migration

(**A**) U87MG and U87MG-EGFR cells transfected (or not) with xCT or EGFR (#1) siRNAs were cultured in glutamate-free medium for 8 h in the absence or presence of 1 μM gefitinib, after which the culture supernatants were assayed for glutamate. Data are means ± SD from four independent experiments. $^{**}p < 0.01$ (Student's *t* test).

(**B**) MGG18 and GB2 cells transfected with control or EGFR (#1) siRNAs were cultured in glutamate-free medium for 8 h, after which the culture supernatants were assayed for glutamate. Data are means ± SD from four independent experiments. $^{*}p < 0.05$, $^{***}p < 0.001$ (Student's *t* test).

(**C**) T98G cells were subjected to a scratch assay in the absence or presence of 200 μM sulfasalazine or 250 μM glutamate for the indicated times and then imaged by phase-contrast microscopy (left panel). The migratory distances of the cells at each time point are presented as means ± SD from three independent experiments (right panel). $^{**}p < 0.01$ versus the corresponding value for nontreated cells (Student's *t* test).

(**D**) U87MG-EGFR cells were assayed for migration toward 5% FBS, EGF (10 ng/ml), Amphiregulin (20 ng/ml), or TGF-α (5 ng/ml) in the absence or presence of 200 μM

sulfasalazine or 250 μM glutamate. Data are means ± SD from three independent experiments. *$p < 0.05$, **$p < 0.01$, ***$p < 0.001$ (Student's t test).

(**E**) MGG18 and GB2 cells were assayed for matrix invasion toward 5% FBS in the absence or presence of 200 μM sulfasalazine or 250 μM glutamate. Data are means ± SD from three independent experiments. *$p < 0.05$, **$p < 0.01$, ***$p < 0.001$ (Student's t test).

(**F**) Schematic representation of the organotypic brain slice culture system.

(**G**) Immunofluorescence analysis of human vimentin for detection of matrix-invading glioma cells in a mouse brain slice. Brain slices implanted with U87MG-EGFR tumor pieces were cultured for 14 days in the absence or presence of EGF (10 ng/ml) or 100 μM sulfasalazine. The white dashed lines indicate the edge of each tumor piece. Scale bars, 100 μm. (**H**) Quantification of matrix invasion determined as in (**G**). The distance between the edge of the tumor piece and the corresponding invasion front formed by the matrix-invading tumor cells was measured. Data are means ± SD from three independent experiments. *$p < 0.05$, **$p < 0.01$ (Student's t test).

(**I**) Kaplan-Meier survival curves for mice with brain tumors derived from implanted U87MG-EGFR cells stably expressing control or xCT shRNAs ($n = 5$ for each group). **$p < 0.01$ (log-rank test).